Computational Studies of Cobalt-Substituted Aluminophosphates†

Neil J. Henson,* P. Jeffrey Hay, and Antonio Redondo

Theoretical Division, Los Alamos National Laboratory, Los Alamos, New Mexico 87545

Received: June 3, 1999; In Final Form: December 17, 1999

Electronic structure calculations have been performed on a number of models for cobalt substituted aluminophosphates (or CoAPOs) using density functional theory. A number of different cluster models of CoAPOs were constructed and used for the calculations. Our results predict that the high-spin forms of cobalt in tetrahedral coordination are the most stable in agreement with previous electron spin resonance measurements. Also, we find that the structural parameters obtained from geometry optimizations are in good agreement with X-ray absorption experiments (EXAFS). For example, for models of CoAPO compounds with cobalt in the reduced Co(II) oxidation state we calculate the Co−O bond length to be ca. 1.94 Å from cluster calculation as compared to 1.90 Å from EXAFS measurements on reduced CoAPO-18. Our calculations also show the necessity of applying constraints when considering cluster models to correctly represent the local environment around the transition metal, and we have developed a method using atomistic shell-model calculations to obtain reasonable constraints for this purpose. We have calculated the thermochemistry of a likely initiation step for partial oxidation with a number of substrates. It is found that the reaction is more favorable when an additional ligand, H_2O or hydroxyl, is introduced into the cobalt coordination sphere forming a five-coordinate local geometry, and that also considerable stabilization of the resulting alkyl radical can be achieved by the formation of a metal−carbon bond. Additionally, it can be noted that although for reproduction of EXAFS data for four-coordinated cobalt models, smaller cluster are sufficient, when considering the energetics of five-coordinated cobalt species, larger cluster are needed to avoid the formation of unrealistic fragment products. We have also investigated the interaction of small molecules (O_2 and CH_3CN) with the cobalt center. Whereas we find no evidence for a stable intermediate involving direct coordination of molecular oxygen, our results with acetonitrile show good agreement with previous EXAFS measurements on CoAPO-5/CH_3CN.

1. Introduction

The introduction of transition metals into zeolites offers the prospect of combining the known proclivities of these elements for heterogeneous catalysis with the shape-selective properties of microporous structures. This area has been the subject of a recent detailed review.[1] Since the first report of the synthesis of aluminophosphate nanoporous materials by Wilson and co-workers in 1982,[2] it has been shown that these structures are particularly suited to the substitution of a wide variety of elements including transition metals.[3] Cobalt has been found to substitute into a large number of aluminophosphate frameworks including AFI, AEL, AFN, AEI, ATV, ATS, AFO and AFY[4] with cobalt aluminophosphate-5 (CoAPO-5) being the most widely studied. Recently, Stucky and co-workers have synthesized a number of microporous cobalt phosphates that could also have promising properties.[5,6] CoAPOs have also been shown as active oxidation catalysts, both homogeneous and heterogeneous, in a wide selection of reactions. For example, CoAPO-5 and Co-APO-11 are able to effect the oxidation of *p*-cresol to *p*-hydroxybenzaldehyde at high selectivity and conversion with molecular oxygen as an oxidant.[7]

Since, for CoAPOs to be effective catalysts, cobalt substitution levels in these materials are needed to be of the order of a few percent, characterization of the cobalt active site has proved to be a challenging problem. For example, there is considerable debate on whether Co(II) or Co(III) is present in the aluminophosphate framework and exactly what the mechanism for oxidation involves during the catalytic process. These are areas in which a theoretical treatment of these systems can contribute.

Several recent theoretical studies on similar systems are of relevance to this work. Márquez and co-workers performed a joint experimental-theoretical study on amorphous aluminophosphate catalyst models. They found that Hartree−Fock calculations on metaphosphate-like clusters appeared to reproduce experimental data well.[8] They note particularly that polarization functions are a necessary component of the basis set required to handle phosphorus atoms correctly in their clusters. Pierloot and co-workers performed density functional theory and multiconfigurational perturbation theory calculations on clusters representing extra-framework Co(II) ions in an aluminosilicate zeolite to rationalize structure and electronic spectra.[9] They find that the presence of cobalt causes significant local distortion around the site and that this causes splitting in the observed spectra rather than Jahn−Teller distortions.

In this paper, we employ a number of theoretical techniques to assess whether quantum mechanical calculations on small clusters are a representative model of cobalt substituted aluminophosphates. Our main focus will be to investigate the effect of cluster size, termination and the use of constraints have on the ability of the calculations to rationalize experimental results. Since the amount of available experimental data on these systems is somewhat limited, we will also focus our comparisons on geometric information obtained by EXAFS measurements on several different CoAPO structures.

† LA-UR 99-2619.

10.1021/jp991798f CCC: $19.00
Published on Web 02/11/2000

2. Theoretical Background

Calculations using density functional theory (DFT) are a rapidly growing choice for the study of many systems using first-principles approaches. They include electron correlation effects which are important for many chemical processes at a similar computational cost to calculations at the Hartree−Fock level of theory. Although the reliability of these methods for small organic molecules has been well established, studies of transition metal containing compounds are less well developed. In particular calculations on paramagnetic systems where a number of spin states are possible provide a particular challenge to the approach.

This work uses the B3LYP hybrid functional, which is a three-parameter hybrid functional which combines the gradient-corrected exchange functional of Becke and the correlation functional of Lee, Yang, and Parr[10,11] with Hartree−Fock exchange. This relatively new method has recently shown promising results, suggesting that it may be preferable to other commonly employed functionals.[12] Geometry optimizations were performed with the Berny analytical gradient method.[13] All calculations were performed with the GAUSSIAN98[14] software.

As will be discussed in greater detail later, most of the calculations are of the all-electron type with the 6-311G all-electron basis set of Wachters and Hay[15,16] for cobalt with various additions. In addition, we employ the following basis sets: 6-31G* on phosphorus and 6-31G on the remaining atoms in the cluster. Recent studies have shown the importance of including a polarization function on phosphorus when performing quantum mechanical calculations on cluster models.[8] Also, our previous work on cobalt coordination complexes has suggested that all-electron basis set on the transition metal is preferred.[17]

Atomistic simulations were carried out with the GULP software and the DIZZY software.[18,19]

More details on these calculations are given in the appropriate sections below.

3. Experimental Background

Cobalt substituted aluminophosphates (CoAPOs) are generally synthesized using standard hydrothermal methods involving the use of a cobalt(II) source (for example, $CoSO_4$) with alumina, phosphoric acid, and an organic molecule that acts as a template for the formation of the microporous framework.[2,3] This generally produces a blue sample which is interpreted as being indicative of the presence of Co(II). During the calcination process to remove the template, a color change to yellow-green is observed which has been interpreted by some to indicate partial oxidation to Co(III).

A wide variety of experimental techniques have been employed to characterize cobalt in aluminophosphates including X-ray powder diffraction,[5,20−22] infrared[23] and, ultraviolet spectroscopies,[24,25] X-ray absorption spectroscopy,[26,27] nuclear magnetic resonance,[28] and electron spin resonance,[29−31] as well as extensive catalytic testing for oxidation reactions.[32−34]

Barrett and co-workers have made extensive studies on cobalt substituted aluminophosphates.[26,27] They find that, depending on the framework and synthesis conditions, a CoAPO sample can contain different type of acid sites. For example, substitution of Co(II) into the $AlPO_4$-5 and $AlPO_4$-36 framework leads to the generation of a predominance of Lewis acid sites, whereas in $CoAlPO_4$-18, Brønsted sites are the important species. In addition, their data is consistent with the cobalt environment in CoAPO-18 being asymmetric consisting of one long and three short Co−O bonds.

Several electron-spin resonance (ESR) studies have been performed on CoAPOs. The earliest studies focused on the CoAPO-5 structure. Iton and co-workers[29] reported that a loss of signal intensity during calcination could be ascribed to oxidation of Co(II) to Co(III) in CoAPO-5 and -34 type materials. In contrast, Wu and co-workers found that no paramagnetic signal could be observed in the calcined form. They also find that the ESR spectra for the reduced CoAPO-5 sample is consistent with a distorted low-spin Co(II) environment.[35] However, other studies have obtained results in conflict with Iton and co-workers. In particular, studies by Kurshev and co-workers[31] and by Wu and co-workers[35] have suggested that a possible alternate explanation of the signal loss is the formation of a diamagnetic cobalt-dioxygen adduct. Wu and co-workers further detected vibrational bands consistent with O−O stretches in the Raman spectrum of a calcined sample of CoAPO-11.[35] For the as-synthesized Co(II) samples, the resonances and lack of hyperfine splitting are consistent with a distorted tetrahedral coordination environment arising from low-spin Co(II).

4. Results and Discussion

4.1. Calculations on Small Cluster Models. Our initial calculations were performed on clusters consisting of a single cobalt atom connected to four adjacent phosphorus tetrahedra terminated with hydrogen atoms. Three models were considered: Co(II), Co(III), and the Brønsted acid site model with Co(II) (denoted as Co(II)−H) (Figure 1). Although the isolated Co(II) model is unlikely to be present in a typical material purely on charge compensation grounds, recent work by Barrett and co-workers[27] has suggested that such a structure may form as a consequence of defect formation.

Convergence of the SCF wave function initially proved difficult, so the following procedure was adopted. The SCF wave function was first converged using a minimal basis set (STO-3G) at the (unrestricted) Hartree−Fock level of theory. This wave function was then used as a guess for an analogous calculation at the B3LYP level of theory. The basis set was then progressively advanced from STO-3G to 3-21G to the final full basis set projecting the previous solution onto the larger basis set to form the guess.

Initially, studies were performed to predict the most energetically favorable spin state for cobalt in each of the models. In the case of Co(III) (d^6) in a regular tetrahedral environment, we would expect the low-spin configuration to be a triplet and a possible high-spin configuration to be a quintet. In addition if a distortion from tetrahedral symmetry occurs, a singlet state is also possible. We considered all three of these cases and performed full geometry optimizations for each. The results are given in Table 1. It can be seen that the most stable spin states for Co(II) and Co(III) are predicted to be the quartet and the quintet respectively which agrees with ESR measurements.

The remainder of the calculations in this paper will use these spin states exclusively unless otherwise stated.

We now focus on the optimized geometries as calculated above. The calculated cobalt−oxygen bond lengths are given in Table 2 and compared to experimental data. The EXAFS measurements of Sankar and co-workers are listed in the table for comparison. CoAPO-18 is a particularly good choice in this case, since the EXAFS measurements suggest that this is one of the few framework structures where complete oxidation to the Co(III) species is possible on calcination. It can be seen that the geometry around Co(II) and Co(III) is quite symmetric with respect to the Co−O bond lengths. Sankar and co-workers have suggested the possibility of a significant Jahn−Teller

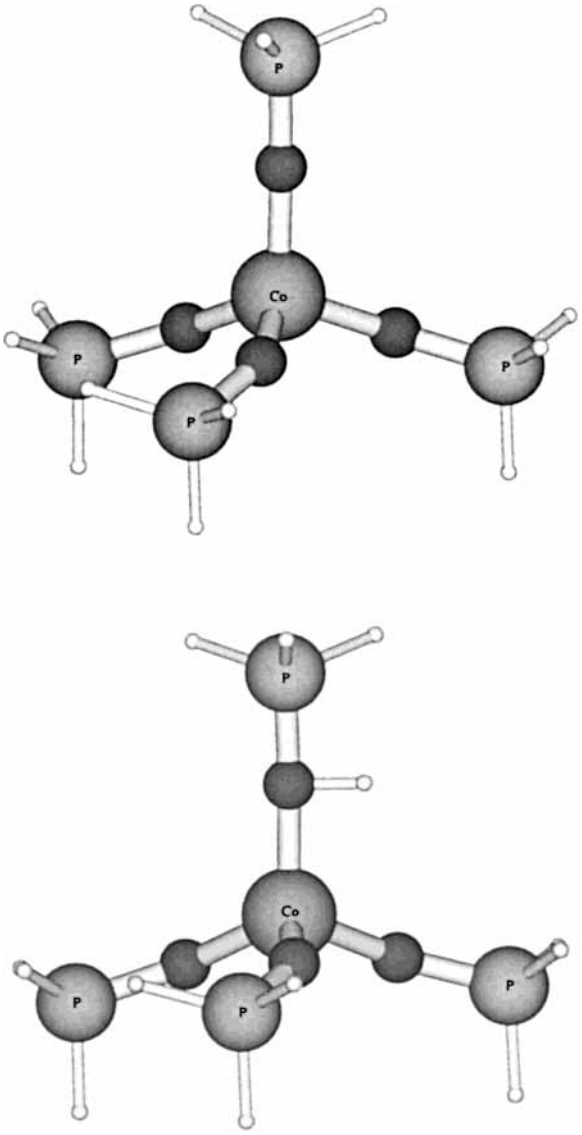

Figure 1. Small cluster models for cobalt aluminophosphates. (a) Co-$(OPH_3)_4^{n+}$ model for Co(II) and Co(III), (b) $Co^{2+}H(OPH_3)_4$ model for Brønsted acid site.

TABLE 1: Results of Spin-State Calculations on Cobalt Models

model	state	relative energy (kJ mol^{-1})
Co(II)	doublet	+115.1
Co(II)	quartet	0.0
Co(II)	sextet	+287.6
Co(III)	singlet	+942.1
Co(III)	triplet	+104.0
Co(III)	quintet	0.0

distortion for the Co(III) d^6 case to account for the EXAFS measurements[26]; we find no evidence for this effect in this set of calculations. Clearly, the values for the Co(II) model give bond lengths in keeping with expectations for tetrahedral Co(II) as well as showing reasonable agreement with the EXAFS results for CoAPO-18. The results for the Brønsted model show considerable distortion as a consequence of the bridging hydroxyl group. This result is similar to that obtained in numerous studies on aluminosilicate clusters.[36] Tetrahedral Co(III) is rarely found in any condensed phase structures, presumably since the ligand-field stabilization energy favors the octahedral coordination environment. It has been reported in the heteropolytungstate structure, $K_5Co^{III}O_4W_{12}O_{36}\cdot 20H_2O$, by

TABLE 2: Results of Geometry Optimizations on Cobalt-Substituted Aluminophosphate Clusters and Their Comparison with Experimental Data

	r (Å)			
model	Co−O	Co−O	Co−O	Co−O
Co(II) H-terminated	1.94	1.94	1.93	1.94
Co(II) in CoO (O_h)	2.13			
Co(II) in Co_3O_4 (T_d)	1.93			
EXAFS:CoAPO-18 reduced[26]	1.90			
Co(II)−H H-terminated	1.98	1.87	1.88	2.27
Co(III) H-terminated	1.84	1.84	1.84	1.85
Co(III) in Co_3O_4 (O_h)	1.92			
Co(III) in tungstate (T_d)	1.88			
EXAFS:CoAPO-18 calcined[26]	1.83			

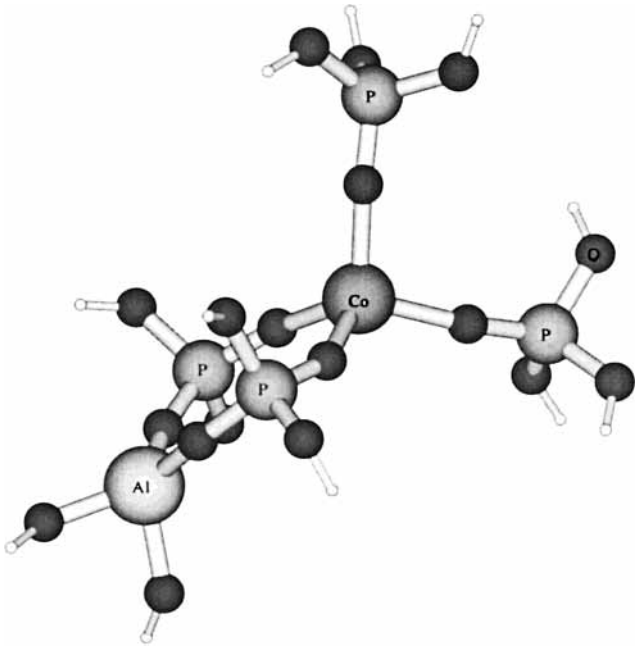

Figure 2. Model for small cobalt cluster with hydroxyl termination, $Co(OP(OH)_3)_2(OP(OH)_2)_2(AlO_2(OH)_2)^{n+}$.

Baker and co- workers[37] who report a bond length of 1.88 Å. However, the crystal structure is poorly defined so there is some uncertainty about this number.

Although termination of clusters with hydrogen is a popular approach mainly due to the relative computational requirement, many workers have criticized this approach due to the large electronegativity difference between hydrogen and oxygen. The alternative termination scheme is to use hydroxyl groups. To investigate the effect of varying termination models in this system we also performed the same geometry optimization calculations detailed above with hydroxyl termination. For these cluster models, terminating with hydroxyl groups requires the inclusion of an (aluminum) tetrahedron in the model to prevent overlapping atoms as shown in Figure 2. The results of the geometry optimizations are given in Table 3.

One of the disadvantages of using hydroxyl termination is that it can lead to unrealistic hydrogen bonds forming between terminating atoms which can often distort the cluster geometry in such a way as to make the local environment around the region of interest unrealistic.

4.2. Calculations on Large Cluster Models. To assess whether there is any dependence on cluster size for the geometric parameters calculated in the previous section, we constructed a series of larger models which consisted of the previously studied

TABLE 3: Results of Geometry Optimizations on Cobalt-Substituted Aluminophosphate Clusters Terminated with Both Hydrogen and Hydroxyl

	r (Å)			
model	Co−O	Co−O	Co−O	Co−O
Co(II) H -terminated	1.94	1.94	1.93	1.94
Co(II) OH-terminated	1.93	1.94	1.95	1.99
Co(II)−H H-terminated	1.87	1.88	1.98	2.27
Co(II)−H OH-terminated	1.89	1.90	1.92	2.20
Co(III) H-terminated	1.84	1.84	1.84	1.85
Co(III) OH-terminated	1.84	1.84	1.87	1.87

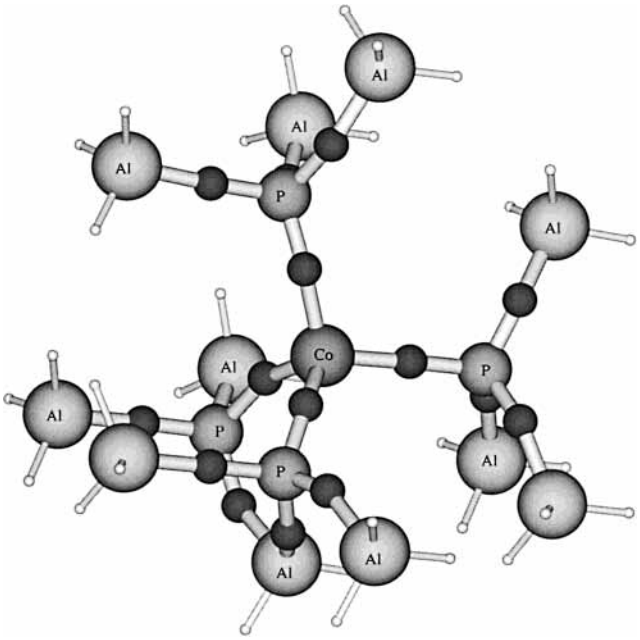

Figure 3. Large cluster model for cobalt aluminophosphates, $Co^{n+}O_{16}$-$Al_{11}P_4H_{32}$.

TABLE 4: Results of Minimizations of Larger Clusters Showing a Comparison with Bond Lengths Obtained for Smaller Clusters

	no. of Al/PO_4	*r* (Å)			
model	coordination shells	Co−O	Co−O	Co−O	Co−O
Co(II)	1	1.94	1.94	1.93	1.94
Co(II)	2	2.05	2.05	2.06	2.10
Co(II)−H	1	1.87	1.88	1.98	2.27
Co(II)−H	2	1.92	1.94	2.03	2.31
Co(III)	1	1.84	1.84	1.84	1.85
Co(III)	2	1.91	1.93	1.93	1.94

clusters with an coordination sphere of tetrahedra added. An example of such a larger cluster is illustrated in Figure 3. Geometry optimizations were performed on these clusters with no constraints applied. The results for these optimizations are given in Table 4; the bond lengths for the smaller clusters are also reproduced for comparison. It can been seen that there is significant lengthening of the Co−O bond in both the Co(II) and Co(III) models when we move to the larger cluster. This lack of consistency between the different sized models combined with the poorer agreement of the larger cluster results with the EXAFS data suggests that the good agreement observed for the smaller models may have been fortuitous. This problem will be addressed further in the next section.

4.3. Cluster Calculations with Constraints. One possible deficiency in the models detailed in earlier sections is the lack of structural constraints placed on the cluster geometry. In the unconstrained systems, the clusters may adopt geometries that do not adequately represent those in bulk materials. Previous workers have addressed this issue by placing constraints on the structural minimization. This has been generally implemented by either fixing several bond lengths or bond angles, or by fixing the positions of atoms in the periphery of the cluster. We will adopt the second approach here. Since there is a significant difference between the ionic radii of Al^{3+} and $Co^{2+/3+}$ (Al^{3+}: 0.535 Å, Co^{2+}: 0.745 Å, Co^{3+}: 0.61 Å),[38] we cannot simply look to the structure of a parent aluminophosphate structure for our constraints, since this would undoubtedly place considerable strain on the system. Instead, we look to the method of atomistic simulation to derive suitable starting models for our cluster calculations.

Atomistic simulation methods particularly using the shell model have been well developed by a number of groups, especially in the case of condensed phase oxides and zeolites.[39−41] The generalized form of the potential used in these models consists of a Buckingham potential combined with an electrostatic term

$$E_{ij} = A_{ij} \exp\left(-\frac{r_{ij}}{\rho_{ij}}\right) - \frac{C_{ij}}{r_{ij}^6} - \frac{q_i q_j}{r_{ij}} \qquad (1)$$

where r_{ij} is the distance between two ions i and j, with charges q_i and q_j, and A_{ij}, ρ_{ij}, and C_{ij} are fitted parameters.

In the specific case of aluminophosphates, several potentials have been derived. Gale and Henson fitted a set of parameters using formal charges to the structure of berlinite[42] and later demonstrated their applicability to a wide range of different aluminophosphates.[43] Also, there have been two potentials fitted to ab initio potential energy surfaces calculated from quantum mechanical calculations on clusters.[44,45] Lewis and Catlow fitted both rigid ion and shell model potential parameters for a wide range of transition metal oxides;[39] however, since the oxygen charge model differs from our previous work on aluminophosphates, we can only use the rigid ion model here. In addition, the Lewis and Catlow parameters were fitted to the structure of cobalt(II) oxide containing only octahedral aluminum. However, we can derive a suitable value for tetrahedral Co(II), which is more relevant to our aluminophosphate models, using a modified Huggins-Meyer relationship after Lewis and Catlow:[39]

$$A_{\text{tet}} = A_{\text{oct}} \exp(-\Delta r/\rho) \qquad (2)$$

where A_{tet} and A_{oct} are the Buckingham A parameters for tetrahedral and octahedral geometry, respectively, Δr is the difference in ionic radii for the two coordinations, and ρ is a common Buckingham ρ parameter. If the ionic radius of the anion (i.e., O^{2-}) is assumed to be constant, Δr can be expressed as

$$\Delta r = d_{\text{oct}} - d_{\text{tet}} \sim (0.06) r_{\text{oct}} \qquad (3)$$

where r_{oct} is the radius of the ion in octahedral coordination. We also make the gross approximation of neglecting the shell model from the Gale and Henson potential to allow these rigid ion model parameters to be easily incorporated in our model. Since we are only interested in deriving *approximate* starting models for our cluster calculations, this is not a significant problem. Since there were no available potential parameters for Co(III), we performed a fitting procedure to obtain approximate values. As has been mentioned previously, there are few examples of Co(III) in tetrahedral coordination; therefore, we focused on structures with octahedral Co(III). We used the

TABLE 5: Summary of Potential Parameters for Atomistic Simulations

	A_{ij} (eV)	ρ_{ij} (Å)	C_{ij} (eV Å^{-6})
Al−O	1460.3	0.2991	0.0
P−O	877.3	0.3594	0.0
O−O	22764.0	0.1490	27.88
O−O_{OH}	22764.0	0.1490	27.88
Co(II)−O	673.1	0.3372	0.0
Co(III)−O	601.5	0.3372	0.0
Co(II)−O_{OH}	472.5	0.3323	0.0
Al−O_{OH}	2753.7	0.2382	0.0
P−O_{OH}	6177.2	0.2100	0.0
O−H	308.5	0.1001	0.0

	D_e (eV)	a (Å^{-1})	r_0 (Å)
O_{OH}−H	8.378	2.044	0.9

	k_{ijk} (eV rad^{-2})	θ_0
O−Al−O	2.0972	109.47
O−Co(II)−O	2.0972	109.47
O_{OH}−Co(III)−O	2.0972	109.47

	q
Al	+3.0
P	+5.0
O	−2.0
O_{OH}	−1.426
H	0.426

structure of the mixed Co(II)/Co(III) oxide spinel, Co_3O_4[46] with the potential parameters derived above for tetrahedral Co(II). We fixed the charges at their formal values, used the O−O repulsive parameters from Lewis and Catlow, then fitted the parameters for Co(II) and Co(III). The GULP software was used for all the atomistic calculations in this section.[18] The resulting Co(III) parameters were then modified according to eq 3. The resulting values are listed in Table 5. Since a three-body term of the form

$$E_{ijk} = k_{ijk}(\theta - \theta_0) \tag{4}$$

where k_{ijk} is a force constant and θ_0 is the equilibrium angle, is present in the aluminophosphate potential for angles around aluminum, a similar term was added for Co(II) and Co(III) with the same parameters. This provided parameters necessary to perform calculations on Co(II) and Co(III) models. To perform atomistic calculations on Co(II)−H models, we need to obtain further parameters. Using the procedure of Schröder and co-workers,[47]we fitted new parameters necessary to handle the bridging hydroxyl species. An oxygen species (O_{OH}) is added with a charge of −1.426 and interaction parameters with other species derived by further fitting. The O_{OH}−H bond is represented by a Morse potential of the form

$$E_{ij} = D_e(1 - \exp(-a_{ij}(r - r_0)))^2 \tag{5}$$

These parameters also listed in Table 5. Using these parameters, we performed a series of atomistic defect calculations using the approach of Mott and Littleton.[48] Models were derived using the structure of Mora and co-workers[49] with cobalt being substituted at Al(1) as before. In this calculation, the proton is represented as an interstitial hydrogen atom bonded to the bridging oxygen group; the center of the defect cluster being at the cobalt position. All atoms lying within a sphere of radius r_2 of the defect center are treated explicitly, and within an inner sphere of radius r_1 the atoms are allowed to relax anharmonically during the minimization. Outside the r_2 boundary, interactions with the defect are handled more approximately as a dielectric response to the defect charge. Several calculations were performed using increasing values of r_1 and r_2. Using values of $r_1 = 11$ Å and $r_2 = 22$ Å, the energy change on increasing the radii further was found to be less than 0.001 eV for each minimized structure. This corresponds to an inner region of ca. 700 atoms.

TABLE 6: Summary of the Structures of Constrained Minimizations of Cobalt Cluster Models

model	no. of Al/PO_4 coordination shells	termination	r (Å) Co−O	Co−O	Co−O	Co−O
Co(II)	1	−H	1.91	1.94	1.94	1.95
Co(II)	1	−OH	1.89	1.91	1.93	1.94
Co(II)	2	−H	1.87	1.90	1.92	1.93
Co(II)−H	1	−H	1.84	1.86	1.88	2.17
Co(II)−H	1	−OH	1.86	1.86	1.87	2.10
Co(II)−H	2	−H	1.87	1.86	1.91	2.09
Co(III)	1	−H	1.79	1.87	1.83	1.86
Co(III)	1	−OH	1.81	1.80	1.85	1.85
Co(III)	2	−H	1.81	1.84	1.85	1.87

After geometry optimization of models for Co(II), Co(III), and Co(II)−H, clusters were constructed and quantum mechanical calculations performed as detailed previously. In each case, the capping atoms (−H or −OH) were fixed in space during the minimization procedure. The geometrical parameters of the minimization clusters are summarized in Table 6.

It can be seen that with the constraints applied, there is a much better consistency between the small and large shell clusters than was observed without constraints, and that there is still a good agreement with the EXAFS data. Once again, the choice of termination does not appear to be significant.

4.4. Reactivity with Small Molecules: Thermochemistry. Several mechanisms have been proposed to account for the catalytic activity of CoAPOs. Sheldon and co-workers have classified the reactivity of transition-metal substituted zeolites as occurring by any of three different mechanisms.[7] In the case of cobalt substituted systems, the partial oxidation reaction is thought to occur via a free-radical pathway. For example, in the oxidation of cyclohexane to cyclohexanol and cyclohexanone Lin and co-workers identify a likely initiation step as[32]

$$RH + Co^{III} \rightarrow R^{\bullet} + Co^{II} + H^+ \tag{6}$$

Iton and co-workers proposed a similar initiation step in their study of the oxidation of methanol to formaldehyde.[29] To further assess the validity of our cluster models for simulating CoAPOs we have performed calculations focusing on the energetics of the radical initiation process. It is assumed that the proton generated in the initiation step coordinates to an oxygen adjacent to the cobalt forming a Brønsted acid site. We consider several different possible reaction pathways. In the first set of calculations, we consider the H-terminated two-coordination sphere CoAPO clusters previously optimized, and in particular the constrained energy minimizations performed. Assuming that the initiation step produces free alkyl radicals, we calculated the minimized energies of the parent hydrocarbon and the alkyl radical using the B3LYP functional with a 6-31G* basis set. The reaction energy for the initiation step, ΔE_s can be then be written as

$$E_s = E_{Co^{III}-H} + E_{R^{\bullet}} - (E_{Co^{III}} - E_{RH}) \tag{7}$$

where $E_{Co^{II}}$ is the energy of the optimized Brønsted site model, $E_{R^{\bullet}}$ is the energy of the optimized alkyl radical species, $E_{Co^{III}}$ is the energy of the optimized Co(III) model, and E_{RH} is the

TABLE 7: Results of Thermodynamic Calculations for Small Molecules with Cobalt Cluster Models

	ΔE (kJ mol^{-1})			
R	four-coordinate	five-coordinate (OH)	five-coordinate (H_2O)	cobalt alkyl
methyl	264	82.1	134	58.4
ethyl	215	32.0	84.8	24.7
methoxy	192	9.2	61.2	8.5
cyclohexyl	199	16.1	69.7	15.3

energy of the optimized alkane, respectively. A number of R groups were considered: methyl, ethyl, methoxy and cyclohexyl. The results are presented in Table 7. For this initiation reaction to be favorable, the considerable energy required to effect homolytic C−H fission needs to be offset by the reduction of the Co(III) to Co(II) and the binding of a proton. It can be seen from the table that roughly half of the energy is recovered (experimental C−H bond energy in CH_4 is 435 kJ mol^{-1},[50] calculated with 6-31G* basis set with the B3LYP functional: 472 kJ mol^{-1}) but that the heat of reaction remains highly positive, and unfavorable.

Since it is known that both Co(II) and Co(III) are able to accommodate higher coordination numbers that four, we decided to explore the effect of having a fifth ligand coordinated to the cobalt center on this reaction. We considered two possibilities: a hydroxyl group and a water molecule. Since the constraints that we employed in previous calculations are invalidated by the presence of a fifth ligand, the following calculations were performed with no fixed atoms. The starting configuration for the optimization was generated by placing approximately the fifth ligand along a line joining the cobalt atom to the center of one of the faces of the CoO_4 tetrahedron. In all cases, the introduction of the fifth ligand resulted in significant lengthening of the Co−O(H) bond and the expulsion of a H_3P−OH moiety. Since this is an unrealistic consequence of the limited size of our cluster, the calculations were repeated on clusters derived from the larger of our cluster models and the energetics reported in Table 7. It can been seen the introduction of the fifth ligand appears to significantly reduce the heat of reaction, which suggests that five-coordination may place a role in this mechanism.

Another possible source of stabilization is the coordination of the alkyl radical formed to the cluster. Since there are many examples of cobalt forming metal−carbon bonds, coordination to the metal center is a likely candidate. To form the M−C bond and assuming the initial cobalt center is high spin, a likely spin state for the metal alkyl is the triplet. Again as with starting configurations based on the three-coordination shell clusters were used to avoid unrealistic fragments. The initial Co−C distance set to 1.93 Å and a full geometry optimization performed. The optimized structure of the metal alkyl with methyl is shown in Figure 4. The formation of the Co−C bond results in the lengthening of the three Co−O bonds from 1.88 to 1.92 Å. The computed spin density on cobalt shows a reduction of ca. half-an-electron indicating that a partial bond has formed with the alkyl group. The Co−C bond length is found to be 2.02 Å. Although there are no simple cobalt alkyls to which to compare this value, the structure of vitamin B_{12} and other similar compounds feature Co−C σ bonds with Co(II) in a square planar or octahedral geometry. For this class of structures, bond lengths in the range 1.95−2.05 Å are observed.[51−53] The calculated spin density on cobalt is reduced by approximately half-an-electron unit compared with the parent cluster indicating partial bond formation between Co and the methyl group. Similar structural effects are observed for the other hydrocarbons.

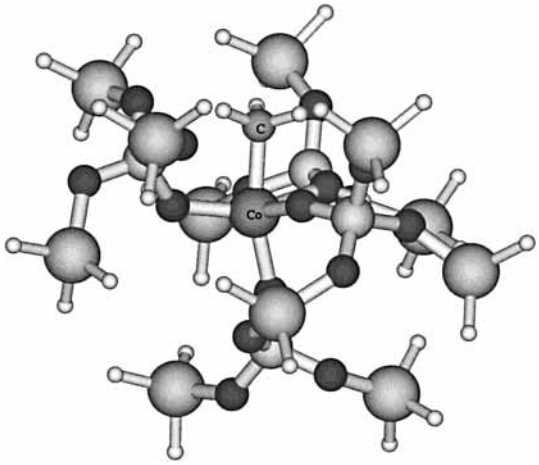

Figure 4. Results of the structural minimization of a methyl alkyl bound to the Brønsted CoAPO model cluster.

4.5. Interaction with Molecular Oxygen. Since CoAPOs have been found to be active catalysts of the partial oxidation of hydrocarbons with molecular oxygen as an oxidant, we now consider possible mechanisms of activation of the catalytic center with this molecule. Wu and co-workers[35] and Kurshev and co-workers[31] contend that their ESR results on CoAPOs during calcination are consistent with species having molecular oxygen directly coordinated to the cobalt center. This mode of binding is reminiscent of that observed in vitamin B_{12}, cobaltoglobin and other mimics of oxygen transport proteins, such as Schiff's bases. We decided to examine the possibility of such species occurring in our small cobalt cluster models. We have recently performed calculations on cobalt Schiff's base coordination complexes with molecular oxygen in order to optimize the basis set required to correctly predict geometries and thermodynamics in these systems.[17] It was found that the following basis set gave good agreement with experimental data using the B3LYP functional: Co (6-311G), O_{ligand} (6-31G), C (6-31G), H (6-31G), and O_2 (6-31+G*), and we will therefore adopt this basis set here.

Taking the optimized structure of the cobalt clusters derived above, we introduced molecular oxygen intersecting approximately the center of the face of the Co(II)O_4 tetrahedron at a distance of 1.89 Å from the cobalt atom, which is similar to that observed in Co(II)(acacen)(O_2)(pyridine). Full geometry optimization was performed. For completeness, we considered both the constrained and unconstrained small clusters, both with −H termination for these calculations. In each case, the oxygen molecule was repelled from the cobalt center and was therefore unbound. We found no evidence for the species observed via infrared spectroscopy by Wu and co-workers.[35]

4.6. Structures with Acetonitrile. Acetonitrile is a popular probe molecule for the investigation of acid sites in small-pore molecular sieves. This mainly because the molecule binds to the framework Brønsted sites resulting in a large shift in a number of characteristic hydroxyl vibrational bands.[27,54−58] In zeolites with divalent metal cations, the acetonitrile molecule has also been found to interact directly with the metal center rather than with the Brønsted site.[55,56] Barrett and co-workers have performed EXAFS and XANES measurements on a number of aluminophosphates and silicoaluminophosphates, and find evidence for several species involving direct interaction of the acetonitrile with the cobalt center.[27]

TABLE 8: Comparison of Calculated and Experimentally Determined Bond Lengths and Bond Angles for Acetonitrile Bound in a Cobalt-Substituted Aluminophosphate

distance/angle	EXAFS (Å, deg)	theory (Å, deg)
Co−O	1.93	1.93
Co−OH		2.09
Co−N	2.05	2.08
Co−C	3.15	3.2
Co−P	3.16	3.18
Co−N−C	180	175

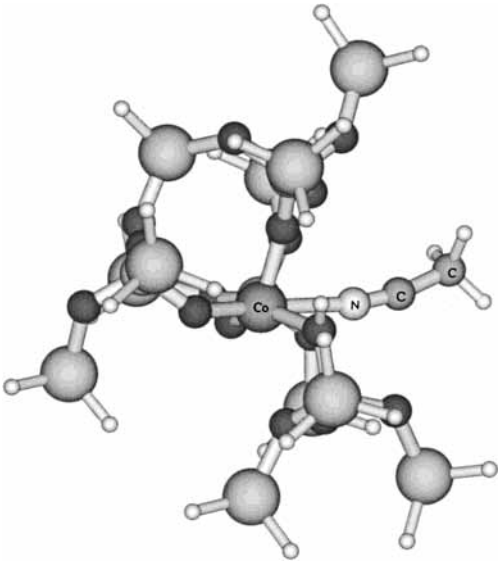

Figure 5. Results of the structural minimization of acetonitrile bound to Brønsted CoAPO model cluster looking down the main AFI channel.

We have performed calculations using our minimized cluster models as a representation for cobalt coordination environment with acetonitrile interacting directly with cobalt and compared our results with the models suggested by the EXAFS and XANES measurements. Barrett and co-workers postulate that the acetonitrile primarily interacts with Co(II) centers, so we constructed a starting model from our previous clusters based on the Co(II) model. Following from our experience with five-coordinated clusters, only the larger of our cluster models was considered. An acetonitrile molecule was coordinated through the center of one of the faces of the CoO_4 tetrahedra at a distance of 1.85 Å. The acetonitrile molecule was oriented such that it would project into the main channel of the AFI structure if the cluster was expanded in size. Again, to allow the necessary expansion of the coordination environment around cobalt, no constraints were placed on the minimization.

The comparison of the bond lengths and bond angles with those measured from EXAFS is given in Table 8. The optimized geometry of the larger cluster is shown in Figure 5. The minimization of the cluster is found to result in an increase in the Co−O(H) bond length. The bond lengths and bond angles agree quite well to those from the EXAFS experiment, which would seem to support the hypothesis that a structure of this type is the predominant species.

4.7. Extra-Framework Cobalt Models. A popular point of contention for transition-metal substituted zeolites is the question of whether the metal ion is located in the framework or in an extra-framework, and presumably, exchangeable site. We decided to examine models for extra-framework species to compare the structural parameters with our previous minimizations with framework models.

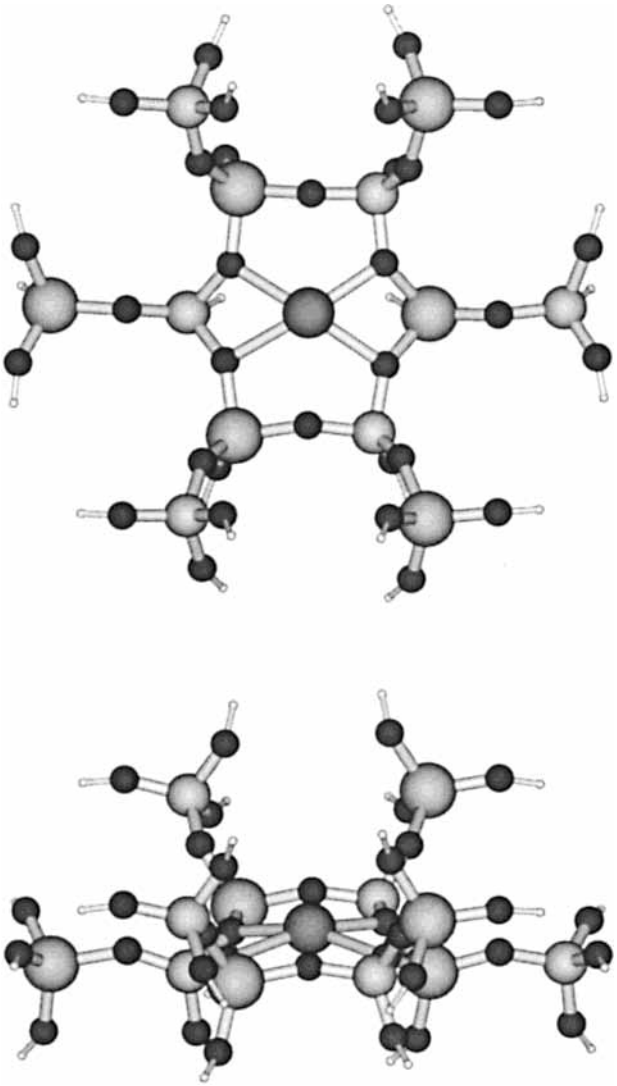

Figure 6. Cluster constructed for extraframework calculation: (a) top view, (b) side view.

Since there is no available crystallographic data on extra-framework metal species in aluminophosphates, we took the atomistic potential parameters fitted in the earlier section and performed a Monte Carlo docking procedure[59] of Co(II) ions in the structure of $AlPO_4$-5[49] to determine likely binding sites. The docking procedure was performed using the DIZZY software.[19] The most favorable site found was located at the center of a six-ring in the wall of the 12-ring channel of the pore structure. This site is similar to the SII site in cation-substituted faujasite zeolites.[60] A structural relaxation was performed using the docked geometry as a starting point using the atomistic simulation method, and then this minimized structure was used to construct a cluster centered on the cobalt cation. The cluster consisted of a single six-ring, with cobalt located at the predicted binding site, with each tetrahedral atom (aluminum or phosphorus) in the ring connected to a single tetrahedral species on one side of the ring and a hydroxyl terminating species on the other. This cluster is illustrated in Figure 6. Since this cluster is significantly larger than those previously detailed, we employed a basis set of reduced quality for this calculation: Co(6-311G), H (STO-3G), O (STO-3G), P (LANL1MB), and Al (LANL1MB) with the effective core potential (ECP) LANL1DZ on P and Al. LANL1MB is a minimum basis set designed to be used specifically with the ECP. A geometry optimization calculation was performed with

GAUSSIAN98 on this cluster using the quantum mechanical method detailed previously.

During minimization, the cobalt cation moves to a more in-plane position (0.06 Å out of plane) and the six-ring expands slightly to accommodate it. The minimized Co−O bond lengths are 1.94−1.96 Å, which are very similar to the bond lengths observed in our framework model clusters. The bond lengths somewhat shorter than is observed in cobalt-substituted aluminosilicate zeolites, such as cobalt-substituted zeolite-A (CoNaA).[61,62] However, although the Co(II) cation in CoNaA is also at the center of a six-ring, the six-ring in the zeolite-A (LTA) framework is considerably different than in the AFI structure. Whereas in LTA the six tetrahedral atoms in the ring are in approximately the same plane and Co(II) is trigonally coordinated at a distance 0.16 Å out of plane, in AFI the ring is such that four atoms lie in a plane and two lie to one side of the plane giving the Co(II) cation four-coordination.

5. Conclusions

We have shown that the combination of hybrid density functional theory and small cluster models can be successfully used to represent cobalt substituted aluminophosphate models. The calculated structural parameters show a particularly good agreement with EXAFS measurements for the smaller cluster models. For larger cluster models, we have illustrated the importance of using a constrained cluster approach; atomistic potentials are useful in deriving appropriate constraint models.

Currently, we are unable to predict any species involving direct coordination of molecular oxygen to the cobalt center, despite the detection of such species in vibrational spectroscopy experiments. Also, we predict a more symmetric environment about cobalt in our calcined models than is measured from EXAFS measurements.

Our calculations on reactivity suggests that the probable initiation step in a typical partial oxidation mechanism of alkanes is likely to involve five-coordinate cobalt, and that the resulting alkyl radical can be stabilized by the formation of a cobalt−carbon bond. Although smaller cluster models consisting of a single set of PO_4 tetrahedra around the central cobalt are sufficient to reproduce experimental bond lengths for CoAPOs, larger clusters are required for a realistic treatment of energetics.

Acknowledgment. The authors thank Richard Martin, Prof. Sir John Meurig Thomas, and Gopinathan Sankar for useful discussion. The work in this paper was carried out under the auspices of the U.S. Department of Energy as part of the UCDRD and LDRD programs at Los Alamos National Laboratory under Contract W-7405-ENG-36.

References and Notes

(1) Hartmann, M.; Kevan, L. *Chem. Rev.* **1999**, *99*, 635.
(2) Wilson, S. T.; Lok, B. M.; Messina, C. A.; Cannan, T. R.; Flanigen, E. M. *J. Am. Chem. Soc.* **1982**, *104*, 1146.
(3) Flanigen, E. M.; Lok, B. M.; Patton, R. L.; Wilson, S. T. In *New Developments in Zeolite Science and Technology*; Murakami, Y., Iijima, A., Ward, J. W., Eds.; Kodansha and Elsevier: New York, 1986.
(4) Meier, W. M.; Olson, D. H. *Atlas of Zeolite Structure Types*, Butterworth-Heinemann, 1992.
(5) Feng, P.; Bu, X.; Stucky, G. D. *Nature* **1997**, *388*, 735.
(6) Feng, P.; Bu, X.; Tolbert, S. H.; Stucky, G. D. *J. Am. Chem. Soc.* **1997**, *119*, 2497.
(7) Arends, I. W. C. E.; Sheldon, R. A.; Wallau, M.; Schuchardt, U. *Angew. Chem., Int. Ed. Engl.* **1997**, *36*, 1144.
(8) Márquez, A. M.; Oviedo, J.; Fernández-Sanz, J.; Benitez, J. J.; Odriozola, J. A. *J. Phys. Chem. B* **1997**, *101*, 9510.
(9) Pierloot, K.; Delabie, A.; Ribbing, C.; Verberckmoes, A. A.; Schoonheydt, R. A. *J. Phys. Chem. B* **1998**, *102*, 10789.
(10) Becke, A. D. *J. Chem. Phys.* **1993**, *98*, 5648.
(11) Lee, C.; Yang, W.; Parr, R. G. *Phys. Rev. B* **1988**, *37*, 785.
(12) Zygmunt, S. A.; Mueller, R. M.; Curtiss, L. A.; Iton, L. E. *J. Mol. Struct. (THEOCHEM)* **1998**, *430*, 9.
(13) Schlegel, H. B. *J. Comput. Chem.* **1982**, *3*, 214.
(14) Frisch, M. J.; Trucks, G. W.; Schlegel, H. B.; Scuseria, G. E.; Robb, M. A.; Cheeseman, J. R.; Zakrzewski, V. G.; Montgomery, J. A.; Stratmann, R. E.; Burant, J. C.; Dapprich, S.; Millam, J. M.; Daniels, A. D.; Kudin, K. N.; Strain, M. C.; Farkas, O.; Tomasi, J.; Barone, V.; Cossi, M.; Cammi, R.; Mennucci, B.; Pomeli, C.; Adamo, C.; Clifford, S.; Ochterski, J.; Petersson, G. A.; Ayala, P. Y.; Cui, Q.; Morakuma, K.; Malick, D. K.; Rabuck, A. D.; Raghavachari, K.; Foresman, J. B.; Cioslowski, J.; Ortiz, J. V.; Stefanov, B. B.; Lui, G.; Liashenko, A.; Piskorz, P.; Komaromi, I.; Gomperts, R.; Martin, R. L.; Fox, D. J.; Keith, T.; Al-Laham, M. A.; Peng, C. Y.; Nanayakkara, A.; Gonzalez, C.; Challacombe, M.; Gill, P. M. W.; Johnson, B. G.; Chen, W.; Wong, M. W.; Andreas, J. L.; Head-Gordon, M.; Repolgle, E. S.; Pople, J. A. GAUSSIAN 98 (Revision A.6); Gaussian, Inc.: Pittsburgh, PA, 1998.
(15) Wachters, A. J. H. *J. Chem. Phys.* **1970**, *52*, 1033.
(16) Hay, P. J. *J. Chem. Phys.* **1977**, *66*, 4377.
(17) Henson, N. J.; Hay, P. J.; Redondo, A. *Inorg. Chem.* **1999**, *38*, 1618.
(18) Gale, J. D. GULP (General Utility Lattice Program); Royal Institution/Imperial College: U.K., 1992−1999.
(19) Auerbach, S. M.; Henson, N. J.; Cheetham, A. K.; Metiu, H. I. *J. Phys. Chem.* **1994**, *99*, 10600.
(20) Chao, K. J.; Sheu, S. P.; Sheu, H. S. *J. Chem. Soc., Faraday Trans.* **1992**, *88*, 2949.
(21) Bontchev, R. P.; Sevov, S. C. *Chem. Mater.* **1997**, *9*, 3155.
(22) Bu, X.; Feng, P.; Stucky, G. D. *Science* **1997**, *278*, 2080.
(23) Marchese, L.; Chen, J. S.; Thomas, J. M.; Coluccia, S.; Zecchina, A. *J. Phys. Chem.* **1994**, *98*, 13350.
(24) Uytterhoeven, M. G.; Schoonheydt, R. A. *Microporous Mater.* **1994**, *3*, 265.
(25) Verbeckmoes, A. A.; Uytterhoeven, M. G.; Schoonheydt, R. A. *Zeolites* **1997**, *19*, 180.
(26) Sankar, G.; Thomas, J. M.; Chen, J. *Nucl. Instrum. Methods Phys. Res., Sect. B* **1995**, *97*, 37. Barrett, P. A.; Sanker, G.; Catlow, C. R. A.; Thomas, J. M. *J. Phys. Chem.* **1996**, *100*, 8977.
(27) Barrett, P. A.; Sankar, G.; Jones, R. H.; Catlow, C. R. A.; Thomas, J. M. *J. Phys. Chem. B* **1997**, *101*, 9555.
(28) Canesson, L.; Boudeville, Y.; Tuel, A. *J. Am. Chem. Soc.* **1997**, *119*, 10754.
(29) Iton, L. E.; Choi, I.; Desjardins, J. A.; Maroni, V. A. *Zeolites* **1989**, *9*, 535.
(30) Xu, R.; Maddox, P. J.; Couves, J. W. *J. Chem. Soc., Faraday Trans.* **1990**, *86*, 425.
(31) Kurshev, V.; Kevan, L.; Parillo, D. J.; Perira, C.; Kokotailo, G. T.; Gorte, R. J. *J. Phys. Chem.* **1994**, *98*, 10160.
(32) Lin, S.-S.; Weng, H.-S. *Appl. Catal. A* **1993**, *105*, 289.
(33) Kraushaar-Czarnetzki, B.; Hoogervorst, W. G. M.; Stork, W. H. J. *Stud. Surf. Sci. Catal.* **1994**, *84*, 1869.
(34) Thomas, J. M.; Raja, R.; Sankar, G.; Bell, R. G. *Nature* **1999**, *398*, 227.
(35) Wu, C. N.; Chao, K. J.; Chang, H.; Lee, L. J.; Naccache, C. *J. Chem. Soc., Faraday Trans.* **1997**, *93*, 3551.
(36) Sauer, J. *Chem. Rev.* **1989**, *89*, 199.
(37) Baker, L. C. W.; Simmons, V. E. *J. Am. Chem. Soc.* **1959**, *81*, 4744.
(38) Shannon, R. D. *Acta Crystallogr.* **1976**, *A32*, 751.
(39) Lewis, G. V.; Catlow, C. R. A. *J. Phys. C.* **1985**, *18*, 1149.
(40) Bush, T. S.; Gale, J. D.; Catlow, C. R. A.; Battle, P. D. *J. Mater. Chem.* **1994**, *4*, 831.
(41) Jackson, R. A.; Catlow, C. R. A. *Mol. Simul.* **1988**, *1*, 207.
(42) Gale, J. D.; Henson, N. J. *J. Chem. Soc., Faraday Trans.* **1994**, *90*, 3175.
(43) Henson, N. J.; Gale, J. D. *Chem. Mater.* **1996**, *8*, 664.
(44) van Beest, B. W. H.; Kramer, G. J.; van Santen, R. A. *Phys. Rev. Lett.* **1990**, *64*, 1955.
(45) Sauer, J.; Schröder, K.-P.; Termath, V. *Collect. Czech. Chem. Commun.* **1998**, *63*, 1394.
(46) Smith, W. L.; Hobson, A. D. *Acta Crystallogr.* **1973**, *B29*, 362.
(47) Schröder, K.-P.; Sauer, J.; Leslie, M.; Catlow, C. R. A.; Thomas, J. M. *Chem. Phys. Lett.* **1992**, *188*, 320.
(48) Mott, N. F.; Littleton, M. J. *J. Chem. Soc., Faraday Trans.* **1938**, *34*, 485.
(49) Mora, A. J.; Fitch, A. N.; Cole, M.; Goyal, R.; Jones, R. H.; Jobic, H.; Carr, S. W. *J. Mater. Chem.* **1996**, *6*, 1831.
(50) Lide, D. R., ed.; *Handbook of Chemistry and Physics*, CRC Press: Boca Raton, 1993.
(51) Lenhart, P. G.; Hodgkin, D. C. *Nature* **1961**, 937.
(52) Kofod, P.; Moore, P.; Alcock, N. W.; Clase, H. J. *J. Chem. Soc., Chem. Commun.* **1992**, 1261.

(53) van Arkel, B.; van der Baan, J. L.; Balt, S.; Bickelhaupt, F.; de Bolster, M. W. G.; Kingma, I. E.; Klumpp, G. W.; Moos, J. W. E.; Spek, A. L.; Spek, A. L. *J. Chem. Soc., Chem. Commun.* **1991**, 225.
(54) Pelmenshikov, A. G.; van Santen, R. A.; Janchen, J.; Meijer, E. J. *J. Phys. Chem.* **1993**, *97*, 11071.
(55) Jänchen, J.; Peeters, M. P. J.; van Wolput, J. H. M. C.; Wothuizen, J. P.; van Hooff, J. H. C.; Lohse, U. *J. Chem. Soc., Faraday Trans.* **1994**, *90*, 1033.
(56) Chen, J.; Thomas, J. M.; Sankar, G. *J. Chem. Soc., Faraday Trans.* **1994**, *90*, 3455.
(57) Kubelkova, L.; Kotrla, J.; Florian, J. *J. Phys. Chem.* **1995**, *33*, 10285.
(58) Meijer, E. J.; van Santen, R. A.; Jansen, A. P. J. *J. Phys. Chem. A* **1999**, *103*, 2553.
(59) Freeman, C. M.; Catlow, C. R. A.; Thomas, J. M.; Brode, S. *Chem. Phys. Lett.* **1991**, *186*, 136.
(60) Mortier, W. J. *Compilation of Extraframework Sites in Zeolites*, Butterworth Scientific Ltd.: Guildford, Surrey, 1982.
(61) Riley, P. E.; Seff, K. *J. Chem. Soc. Chem. Commun.* **1972**, 1287.
(62) Riley, P. E.; Seff, K. *Inorg. Chem.* **1974**, *13*, 1355.